Protein Science (1992), *1*, 1413–1427. Cambridge University Press. Printed in the USA.
Copyright © 1992 The Protein Society

Structure of the oxidized long-chain flavodoxin from *Anabaena* 7120 at 2 Å resolution

S.T. RAO,[1,2] FATHIEH SHAFFIE,[2] CARLOS YU,[2] KENNETH A. SATYSHUR,[2] BRIAN J. STOCKMAN,[3,4] JOHN L. MARKLEY,[3] AND M. SUNDARALINGAM[1,2]

[1] Laboratory for Biological Macromolecular Structure, Department of Chemistry & Biotechnology Center, The Ohio State University, Columbus, Ohio 43210
[2] Crystallography Laboratory, Department of Biochemistry, College of Agricultural & Life Sciences, University of Wisconsin–Madison, Madison, Wisconsin 53706
[3] NMR Laboratory, Department of Biochemistry, College of Agricultural & Life Sciences, University of Wisconsin–Madison, Madison, Wisconsin 53706

(RECEIVED February 13, 1992; REVISED MANUSCRIPT RECEIVED June 1, 1992)

Abstract

The structure of the long-chain flavodoxin from the photosynthetic cyanobacterium *Anabaena* 7120 has been determined at 2 Å resolution by the molecular replacement method using the atomic coordinates of the long-chain flavodoxin from *Anacystis nidulans*. The structure of a third long-chain flavodoxin from *Chondrus crispus* has recently been reported. Crystals of oxidized *A.* 7120 flavodoxin belong to the monoclinic space group $P2_1$ with $a = 48.0$, $b = 32.0$, $c = 51.6$ Å, and $\beta = 92°$, and one molecule in the asymmetric unit. The 2 Å intensity data were collected with oscillation films at the CHESS synchrotron source and processed to yield 9,795 independent intensities with R_{merg} of 0.07. Of these, 8,493 reflections had $I > 2\sigma$ and were used in the analysis. The model obtained by molecular replacement was initially refined by simulated annealing using the XPLOR program. Repeated refitting into omit maps and several rounds of conjugate gradient refinement led to an R-value of 0.185 for a model containing atoms for protein residues 2–169, flavin mononucleotide (FMN), and 104 solvent molecules. The FMN shows many interactions with the protein with the isoalloxazine ring, ribityl sugar, and the 5′-phosphate. The flavin ring has its pyrimidine end buried into the protein, and the functional dimethyl benzene edge is accessible to solvent. The FMN interactions in all three long-chain structures are similar except for the O4′ of the ribityl chain, which interacts with the hydroxyl group of Thr 88 side chain in *A.* 7120, while with a water molecule in the other two. The phosphate group interacts with the atoms of the 9–15 loop as well as with NE1 of Trp 57. The N5 atom of flavin interacts with the amide NH of Ile 59 in *A.* 7120, whereas in *A. nidulans* it interacts with the amide NH of Val 59 in a similar manner. In *C. crispus* flavodoxin, N5 forms a hydrogen bond with the side chain hydroxyl group of the equivalent Thr 58. The hydrogen bond distances to the backbone NH groups in the first two flavodoxins are 3.6 Å and 3.5 Å, respectively, whereas in the third flavodoxin the distance is 3.1 Å, close to the normal value. Even though the hydrogen bond distances are long in the first two cases, still they might have significant energy because their microenvironment in the protein is not accessible to solvent. In all three long-chain flavodoxins, a water molecule bridges the ends of the inserted loop in the β_5 strand and minimally perturbs its hydrogen bonding with β_4. Many of the water molecules in these proteins interact with the flavin binding loops. The conserved β-core of the three long-chain and two short-chain flavodoxins superpose with root mean square deviations ranging from 0.48 Å to 0.97 Å.

Keywords: *Anabaena* 7120; long-chain flavodoxin; oxidation

Flavodoxins mediate electron transfer at low redox potential between prosthetic groups of other proteins (Mayhew & Ludwig, 1975). They consist of a single polypeptide chain (MW range 14–23 kDa) with a tightly bound FMN. The flavodoxin from *Anabaena* 7120, which is produced as with other cyanobacteria, under conditions of limiting iron (Stockman et al., 1988), serves as a mobile electron carrier in transferring electrons from photosystem I to the ferredoxin reductase (Sykes & Rogers, 1984). This same function is taken over by a ferredoxin at higher levels of iron (Tollin & Edmondson, 1980). Just how two very different proteins (a 2Fe–2S ferredoxin and a flavodoxin

Reprint requests to: M. Sundaralingam, Biotechnology Center, #012, 1060 Carmack Road, The Ohio State University, Columbus, Ohio 43210.
[4] Present address: The Upjohn Company, Physical & Analytical Chemistry Division, 301 Henrietta Street, Kalamazoo, Michigan 49001.

with FMN as the cofactor) can play an interchangeable role remains a structural puzzle. In its physiological role, the flavodoxin one-electron chemistry cycles between the semiquinone (sq) and fully reduced (rd) states. However, in contact with air, the flavodoxin is in the fully oxidized state (ox). Binding of the cofactor to the apoprotein alters the FMN reduction potentials for both the ox/sq step, which is 42 mV more positive, and the sq/rd step, which is 253 mV more negative (Paulsen et al., 1990). One objective of flavodoxin structural studies is to understand how the protein fine-tunes these potentials. The structures of two short-chain flavodoxins have been determined in all three oxidation states: that from *Clostridium beijerinckii* (also known as *Clostridium* MP; 138 residues [Burnett et al., 1974; Ludwig & Luschinsky, 1992]) and that from *Desulfovibrio vulgaris* (148 residues [Watt et al., 1991]). *Anabaena* 7120 flavodoxin, which has 169 residues (Leonhardt & Straus, 1989), is a long-chain flavodoxin. The structure of the long-chain flavodoxin from *Anacystis nidulans* (169 residues [Smith et al., 1983; Laudenbach et al., 1987]) is known in the ox state. Its sequence (Laudenbach et al., 1988) differs from that of *A.* 7120 (Leonhardt & Straus, 1989) by 31%. Recently, the X-ray structure of a third long-chain flavodoxin from a eukaryotic red alga *Chondrus crispus*, containing 173 residues, has also been determined in the ox state (Fukuyama et al., 1990). *Anabaena* 7120 is also being studied by NMR spectroscopy (Stockman et al., 1990) so comparisons can be made between the crystal structure and that in solution. We report here the X-ray structure of *A.* 7120 flavodoxin in its ox state at 2 Å resolution.

The characteristic motif of the flavodoxin structures is a five-stranded parallel β-sheet central core with a pair of flanking α-helices. FMN binds at one end of the sheet with its dimethyl benzene edge exposed to solvent. In the long-chain flavodoxins a lobe of about 20 residues is inserted in the middle of the β_5-strand, which has no direct interaction with FMN. An alignment of the *A.* 7120 sequence with that of the *A. nidulans* squence (Fig. 1) shows an insertion of a single residue at the N-terminus and a single deletion at position 29. Of the 52 sequence changes (32%) between the two flavodoxins, 19 are conservative. The sequence of the third long-chain flavodoxin from *C. crispus* (Wakabayashi et al., 1989, Fig. 1) shows a 65% change with that of *A.* 7120, with many insertions and deletions.

FMN can exist in three oxidation states: ox, sq (one electron reduced), and hydroquinone (two electrons reduced, hq). The redox potentials of FMN in the five flavodoxins, whose X-ray structures are known, are compared with those of free FMN in Table 1 (Simondson & Tollin, 1980; Paulsen et al., 1990). It is seen that in the long-chain flavodoxins, E2, the potential for the ox to sq state, is comparable to that of free FMN, whereas E1, the potential for further reduction to the hq state, is much lower in the protein bound form than in free FMN. In all structures, in the ox state, only the hydrophobic edge of the flavin

```
                    1           2           3           4
                    0           0           0           0
                  SSSSSS      HHHHHHHH  HHHHHH    S  SS  SSSS   H
A. 7120         SKKIGLFYGT   QTGKTESVAE  IIRDEFGND-V  VT--LHDVSQAE
A. nidulans      AKIGLFYGT   QTGVTQTIAE  SIQQEFGGESI  VD--LNDIANAD
C. crispus        KIGIFFST   STGNTTEVAD  FIGKTLGAK--  ADAPIDVDDVTD

                    5           6                   7           8
                    0           0                   0           0
                HHHHHH SSS  SSSS                    H  HHHHHH
A. 7120         VTDLNDYQYL  IIGCPTWNIG  EL----QSDW-EGLY  SELDDVDFNG
A. nidulans     ASDLNAYDYL  IIGCPTWNVG  EL----QSDW-EGIY  DDLDSVNFQG
C. crispus      PQALKDYDLL  FLGAPTWNTG  ADTERSGTSWDEFLY  DKLPEVDMKD

                              1           1           1
                    9         0           1           2
                    0         0           0           0
                SSSSSSS SS          H  HHHHHHHHHH        SSS
A. 7120         KLVAYFG-TGD  QIGYADNFQD  AIGILEEKIS  QR---GGKTVGYW
A. nidulans     KKVAYFG-AGD  QVGYSDNFQD  AMGILEEKIS  SL---GSQTVGYW
C. crispus      LPVAIFG-LGD  AEGYPDNF--  -CDAIEEIHD  CFAKQGAKPVGFS

                    1           1           1           1
                    3           4           5           6
                    0           0           0           0
                                        SSS         HHHHHHHHHH
A. 7120         STDGYDFNDS  KALRNGKFVG  LALDEDNQSD  LTDDRIKSWV
A. nidulans     PIEGYDFNES  KAVRNNQFVG  LAIDEDNQPD  LTKNRIKTWV
C. crispus      NPDDYDYEES  KSVRDGKFLG  LPLDMVNDQI  PMEKRVAGWV

                    1
                    6
                    9
                HHHHHHHH
A. 7120         AQLKSEFGL
A. nidulans     SQLKSEFGL
C. crispus      EAVVSETGV
```

Fig. 1. Comparison of the sequence of *Anabaena* 7120 (top line), *Anacystis nidulans* (middle line), and *Chondrus crispus* (bottom line) flavodoxins. The residue numbering corresponds to *Anabaena* 7120. The alignment of *C. crispus* sequence with *A. nidulans* is after Wakabayashi et al. (1989). The sheet and helical regions in *A.* 7120 are denoted as S and H, respectively.

Table 1. *Redox potential values (mv) of flavodoxins at pH 7.0*

Species	E2 (ox/sq)[a]	E1 (sq/hq)
Anabaena 7120	−196	−425
Anacystis nidulans	−220	−415
Chondrus crispus	−222	−370
Desulfovibrio vulgaris	−103	−438
Clostridium beijerinckii	−92	−399
Free FMN	−238	−172

[a] ox, oxidized; sq, semiquinone; hq, hydroquinone.

ring (C7/C8 methyl groups) is exposed to the solvent, whereas the rest of the flavin ring, including the active center N5, is inaccessible to solvent. The crystal structures of *D. vulgaris* (Watt et al., 1991) and *C. beijerinckii* (Smith et al., 1977), determined in all three oxidation states, shows a conformational change in the 57–62 loop of the protein upon reduction from the ox to sq state, flipping the peptide residue (Gly 57 in *C. beijerinckii* and Gly 61 in *D. vulgaris*) so that the carbonyl oxygen engages in a hydrogen bond with the reduced N5H of flavin. Smaller conformational changes are seen on further reduction from the sq to hq state. In spite of the structural data, it has not been possible to fully correlate the redox potentials with the protein environment of FMN or to obtain insights into the actual pathway of electrons to the flavin ring. The existence of the hydrogen bond to N5 in the long-chain flavodoxins in the ox state, in contrast to the short-chain flavodoxins, suggests a rationale for the E2 values of these flavodoxins being comparable to that of free FMN.

Results and discussion

The Ramachandran (ϕ, ψ) plot for the structure is shown in Figure 2, where the glycine residues are shown as squares and other residues as crosses. The conformations of the residues fall within the regions occupying the α_R and β regions and the turns that connect these regions. Four residues are found in the left-handed α_L region: Asn 58 and Ile 59 of the reverse loop, Gln 99, and Asn 135. Of the 19 glycines, 9 are in left-handed regions with 8 in α_L and 1 in β_L.

The average temperature factors (B-values) for the atoms of the various residues are shown in Figure 3. The mean value for the entire structure is only 10 Å^2. The B-values are high in the loop between the α_1-helix and β_2-strand, in the rather loosely structured 3_{10}- and α_2-helices, and in a few residues at either termini. The region with the highest B-value is in the α_1–β_2 loop, where the electron density is ill-defined. In the other two regions with high B-values, the electron density was sufficiently defined to permit a chain trace.

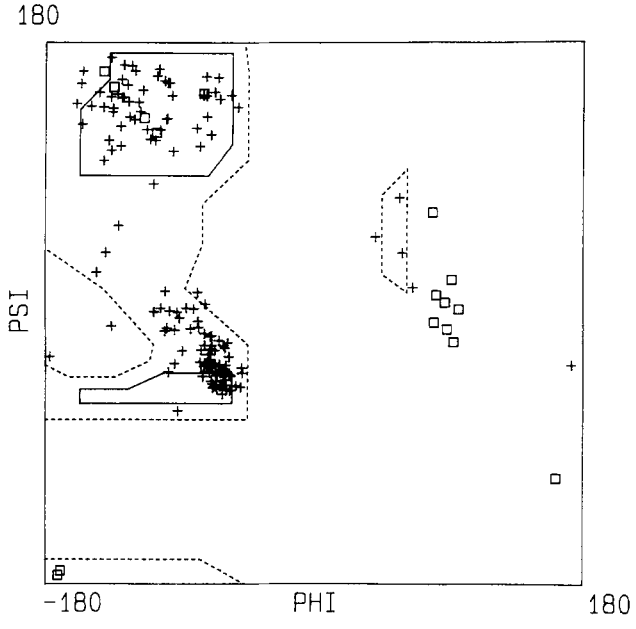

Fig. 2. Ramachandran plot for *Anabaena* 7120. Glycine residues are shown as squares and non-glycyl residues as crosses.

Overall description of secondary and tertiary structure

A ribbon plot (Priestle, 1988) of the molecule is shown in Figure 4 (see also Kinemage 1). The structure is built around a five-stranded parallel β-sheet core with a pair of helices flanking on either side, typical of nucleotide binding folds (Rossmann et al., 1975). FMN binds at the southern edge of the molecule and interacts with residues in the loops between the strands and with the N-terminal residues of the α_1-helix. Residues 4–9, 30–36, 48–54, 81–89, and 115–117/141–143 are involved in the five β-strands. In the fifth strand, the long extra loop is an insertion between residues 117 and 141 (Kinemage 2) and contains a short antiparallel sheet hydrogen bonding between residues 120 and 138. Residues involved in the he-

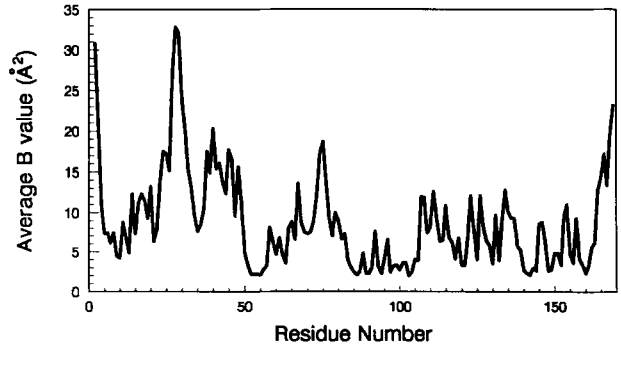

Fig. 3. Average temperature factor (B-value) for various residues in *Anabaena* 7120 flavodoxin. The average value for all residues is 10 Å^2

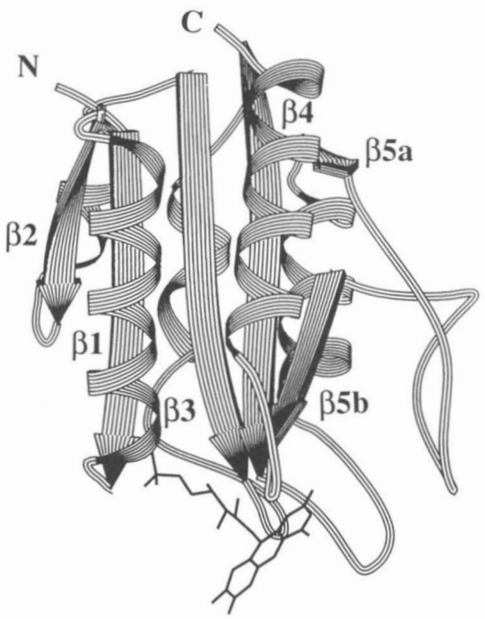

Fig. 4. Ribbon diagram of *Anabaena* 7120 flavodoxin. The bound FMN is also shown. The N- and C-terminii are labeled as are the β-sheets. The two parts of β_5 are labeled 5a and 5b.

lical regions are: 13–26 (α_1), 40–46 (3_{10}), 70–76 (α_2), 100–110 (α_3), and 151–168 (α_4). A summary of the hydrogen bond lengths in these regions is given in Table 2, along with the hairpin loops in the structure. It is seen that the α_2-helix is essentially another 3_{10}-helix, and intermolecular interactions in the crystal may be responsible for this distortion (see below). Intramolecular hydrogen bonds in this structure involving side chain atoms are given in Table 3. There are 10 hydrogen bonds between side chain and backbone atoms and 24 hydrogen bonds among the side chain atoms.

Comparison with other flavodoxin structures

Because it was possible to solve the present structure by molecular replacement with a model of *A. nidulans*, it is not surprising that the two structures are very similar. All the backbone atoms of the two flavodoxin structures are superposable with a root mean square (rms) deviation of 0.84 Å. The α-carbon atoms have an rms deviation of 0.69 Å; a plot of these α-carbon distances is shown in Figure 5, and a superposition of the two structures is shown in Figure 6A. Three regions contain deviations of more than 1 Å: (1) residues 27–30 in the loop region between α_1 and β_2, where the electron density is poorly defined in both cases and which contains the one-residue deletion Ser 29 in the sequence alignment (Fig. 1); (2) residues 70–76 of the α_2-helix, which has an intermolecular interaction with Arg 112 in *A.* 7120 and is almost 3_{10} in character; and (3) residues 132–136 in the long loop, where it turns around and the intermolecular interactions are different in the two cases. Apart from these differences,

Table 2. *Summary of secondary structure hydrogen bonds*

	First O...N H bond	Last O...N H bond	Range of O...N distance (Å)	Mean distance (Å)
Helix				
α_1	13...17	22...26	3.0–3.3	3.1
3_{10}	40...43	43...46	2.9–3.3	3.1
α_2 (3_{10})	70...73	73...76	3.1–3.4	3.2
α_3	100...104	106...110	2.8–3.2	3.0
α_4	151...154	164...168	2.8–3.4	3.0
Sheet				
β_2–β_1	30(O)...4(N)	36(N)...8(O)	2.7–3.1	2.9
β_1–β_3	5(N)...49(O)	9(N)...53(O)	2.8–3.2	3.0
β_3–β_4	48(O)...82(N)	54(N)...86(O)	2.8–3.2	3.0
β_4–β_5	81(O)...115(N)	83(O)...117(N)	2.9–3.2	3.0
	85(O)...141(N)	89(N)...143(O)	2.9–3.2	3.0

Residues	$(\phi,\psi)_2$ (°)	$(\phi,\psi)_3$ (°)	O(i)...N($i+3$) distance (Å)	Type
Hairpin turns				
24-Asp-Glu-Phe-Gly-27	−69/−35	−71/−35	3.5	III
36-Val-Ser-Gln-Ala-39	−66/−25	−106/0	3.5	I
70-Tyr-Ser-Glu-Leu-73	−68/−15	−96/1	3.1	I
78-Phe-Asn-Gly-Lys-81	−51/137	89/−10	3.0	II
97-Asn-Phe-Gln-Asp-100	−69/120	66/18	3.3	II
122-Thr-Asp-Gly-Tyr-125	−74/145	97/3	3.4	II
130-Ser-Lys-Ala-Leu-133	−77/−10	−89/−4	3.5	I
134-Arg-Asn-Gly-Lys-137	60/41	80/−6	3.2	I′
149-Ser-Asp-Leu-Thr-152	−69/−24	−92/−12	3.2	I

Table 3. *Intramolecular hydrogen bonds involving side chain atoms*

Side chain		Backbone		Distance (Å)
OG1	10 Thr	N	13 Gly	3.1
OG1	56 Thr	N	101 Ala	2.9
OD2	90 Asp	N	93 Gln	3.0
OE1	91 Gln	N	126 Asp	2.8
OD2	100 Asp	N	131 Lys	2.9
NH2	112 Arg	O	74 Asp	2.6
OH	125 Tyr	O	142 Ala	2.9
OG	130 Ser	O	98 Phe	2.7
OD1	144 Asp	N	147 Asn	2.8
NE1	159 Trp	O	118 Gly	2.9
Side chain		**Side chain**		**Distance (Å)**
OH	8 Tyr	OE1	16 Glu	3.0
NE2	11 Glu	OG	64 Ser	2.8
NZ	14 Lys	OE1	145 Glu	2.8
		OE2	145 Glu	2.8
OG1	15 Thr	OG1	88 Thr	2.6
OE2	25 Glu	NZ	157 Lys	2.6
NE2	34 His	OH	47 Tyr	2.7
OE1	48 Glu	NZ	81 Lys	2.6
OD2	74 Asp	NZ	108 Lys	2.6
NE2	91 Gln	OD2	144 Asp	3.0
		OE1	148 Gln	3.1
OD2	96 Asp	ND2	128 Asn	3.0
ND2	97 Asn	OD1	100 Asp	2.9
OE1	106 Glu	NH1	134 Arg	2.6
OE2		OG1	116 Thr	2.9
NZ	108 Lys	OE1	111 Gln	2.5
OG	110 Ser	NH1	134 Arg	2.6
OH	119 Tyr	ND2	135 Asn	2.7
NE1	120 Trp	OH	125 Tyr	3.0
OD1	144 Asp	ND2	147 Asn	3.0
OD2	144 Asp	ND2	147 Asn	3.0
OE1	145 Glu	OG1	152 Thr	2.9
OE1	148 Gln	NH1	155 Arg	2.6
NE2	162 Gln	OE2	166 Glu	2.9

the two structures are very similar. A superposition of the sheet regions only of the *A.* 7120 and the *C. crispus* flavodoxin structure gives an rms deviation of 0.51 Å for the α-carbon atoms. The *Chondrus crispus* flavodoxin sequence contains many insertions and deletions compared to *A.* 7120, which occur mostly in the loop regions; it also contains nine additional proline residues distributed throughout the sequence. One hundred twenty-three α-carbons were established as structurally equivalent by inspection of the two models initially superposed using the sheet regions (Fig. 6B), and the rms deviation for these 123 atoms is 0.97 Å. The most significant deviations occur in the short helical region connecting β_2 and β_3 and in the long loop. In Figure 6C and D, the two short-chain flavodoxins are superposed on the *A.* 7120 long-chain flavodoxin using the residues in the β-sheets for the alignment. The rms deviations for the α-carbons were 0.77 Å

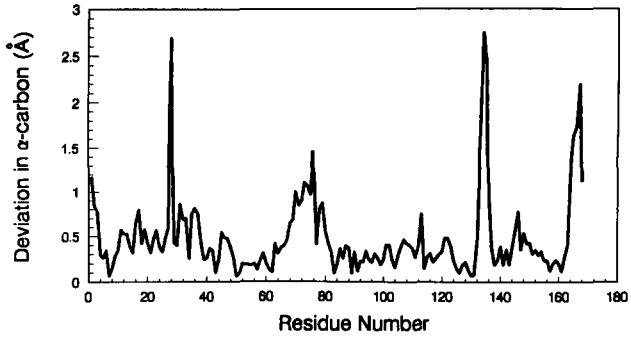

Fig. 5. Plot of the deviation in the α-carbon atoms of corresponding residues in *Anabaena* 7120 and *Anacystis nidulans*. Large deviations are at residues 27–30 (loop region without clear electron density in both structures), 70–75 (α^2-helix), and 132–136 (long loop).

and 0.81 Å for the *C. beijerinckii* (Fig. 6C) and *D. vulgaris* (Fig. 6D) structures, respectively. The figure shows how the insertion of the long loop essentially leaves the two halves of the β_5-strand in alignment, with the short-chain structures lacking this loop. It is interesting that the flanking helices of the *D. vulgaris* structure are more in alignment with the long-chain structures than those of *C. beijerinckii*, which show a lateral shift of about 1 Å. The orientation of the flavin ring is similar in these structures except in *C. beijerinckii*, where it is tilted.

FMN interactions

The interactions of FMN with the protein atoms and water molecules of *A.* 7120 are listed in Tables 4 and 5. The environment of FMN in *A.* 7120 is shown in Figure 7A and Kinemage 3. The FMN is tightly bound to the protein with a number of interactions between the anionic phosphate oxygen atoms, ribityl hydroxyls, and the pyrimidine portion of the alloxazine ring. The alloxazine ring itself is planar within the limits of experimental error.

The phosphate group binds near the N-terminal end of helix α_1 stabilizing the helix dipole. The anionic phosphate oxygen atoms interact with the N-terminal residues of the helix and with atoms in residues in the loop preceding the helix. The hydrogen bond OG1 (Thr 10)...N (Gly 13) stabilizes the phosphate binding loop. The phosphate oxygen OP2 also hydrogen bonds with NE1 of Trp 57, which forms one face of the flavin aromatic sandwich. The ribityl hydroxyl groups interact with either backbone or side chain atoms of residues at or near the C-terminal ends of the three β-strands 3, 4, and 5. Although some of the above interactions involve atoms from protein side chains and are sequence specific, the atoms on the alloxazine ring interact only with backbone atoms of the reverse 58–62 loop between (β_3, α_2) and the 90–99 loop between (β_4, α_3). The amide N of Asp 90 forms a bifur-

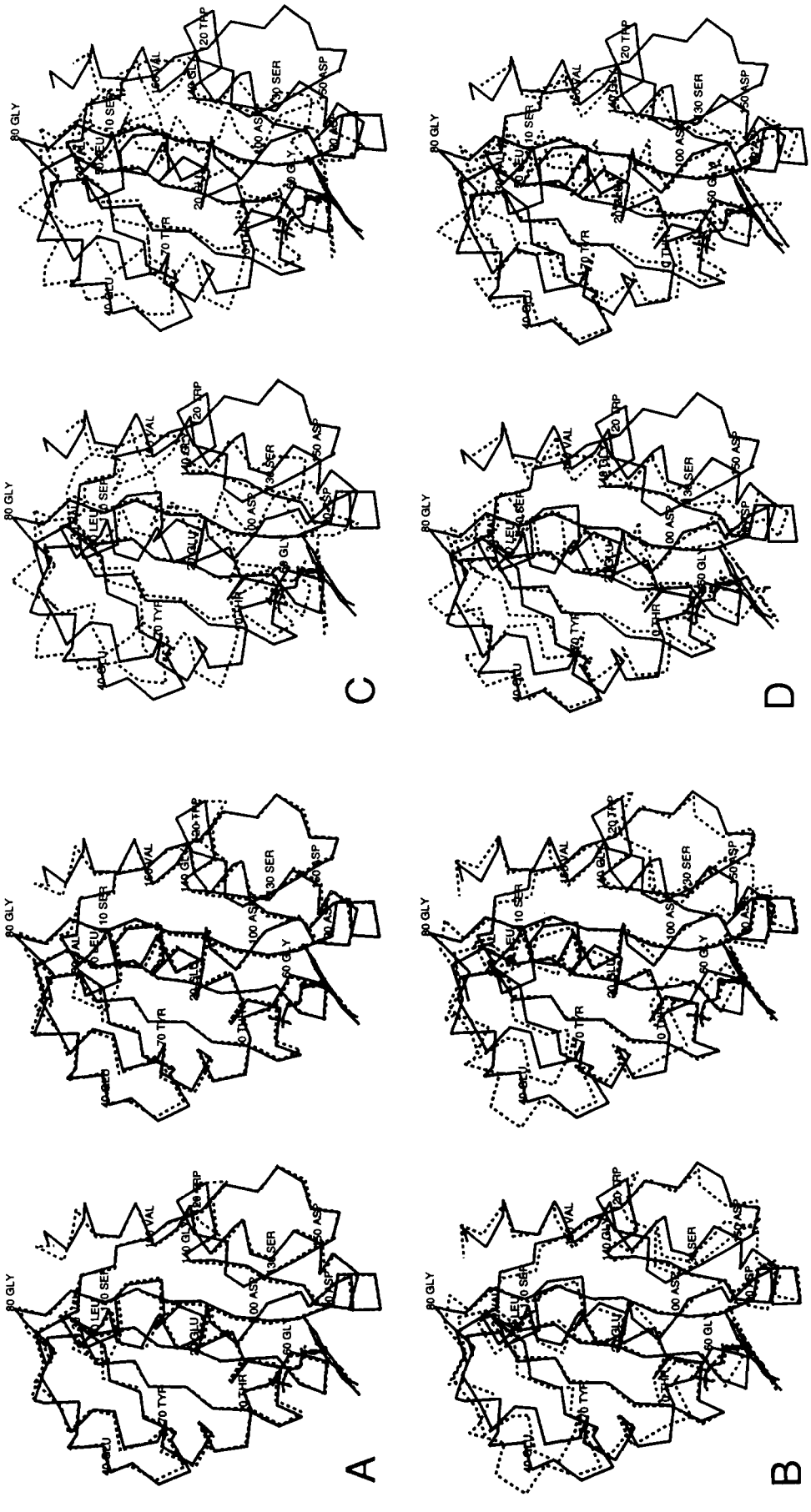

Fig. 6. Stereo diagrams of pairwise superposition of the α-carbon trace of *Anabaena* 7120 flavodoxin (solid line) on the other four flavodoxin structures (dashed line). The bound FMN is also shown: **A**, on *Anacystis nidulans*; **B**, on *Chondrus crispus*; **C**, on *Clostridium beijerinckii*; and **D**, on *Desulfovibrio vulgaris*. The long loop inserted in the middle of the β_5-strand is on the right. Notice that the orientation of the flavin ring is different in *C. beijerinckii*. The coordinates used are the Protein Data Bank entries 2FCR (*C. crispus*), 1FXN (*C. beijerinckii*), and 1FVN (*D. vulgaris*).

Table 4. *Comparison of FMN interactions in the three long-chain flavodoxins*

FMN atom	*Anabaena* 7120			*Anacystis nidulans*[a]			*Chondrus crispus*		
N1	3.0 Å	N	(90 Asp)	3.1 Å			3.1 Å	N	(94 Asp)
O2	3.3	N	(90 Asp)	3.2			3.0	N	(94 Asp)
	2.9	N	(99 Gln)	3.2			2.9	N	(103 Cys)
	2.9	W249		–			–		
N3	2.9	O	(97 Asn)	2.9			2.8	O	(101 Asn)
O4	2.8	N	(60 Gly)	2.7			3.1	OG1	(58 Thr)
N5	3.6[b]	N	(59 Ile)	3.5[b]			3.1	OG1	(58 Thr)
O2′	2.8	O	(56 Thr)	2.6			2.8	O	(55 Thr)
O3′	2.9	OD1	(146 Asp)	2.7			–		
	3.1	W304		3.0	W174		2.8	W247	
O4′	3.1	OG1	(88 Thr)	2.8	W181		–		
	3.4	W272		2.7	W173		3.1	W236	
	–			2.8	W181		3.1	W247	
OP1	2.6	OG1	(12 Thr)	2.6			2.5	OG1	(10 Thr)
	3.1[c]	N	(12 Thr)	3.0[c]					
	3.2	N	(13 Gly)	3.0					
	2.8	N	(14 Lys)	2.8	N	(Val)	2.7	N	(12 Asn)
	–			–			2.7	ND2	(12 Asn)
OP2	3.0	N	(11 Gln)	2.8			2.8	N	(9 Ser)
	3.1	N	(12 Thr)	3.2			2.9	N	(10 Thr)
	3.0	NE1	(57 Trp)	2.9			2.8	NE1	(56 Trp)
OP3	2.7	OG1	(10 Thr)	2.6			2.5	OG1	(8 Thr)
	2.7	N	(15 Thr)	2.9			2.9	N	(13 Thr)
	2.7	OG1	(15 Thr)	2.9			2.6	OG1	(13 Thr)

[a] The interacting residues are the same as in *A.* 7120 except for 14 Val(Lys) and 88 Ala(Thr). In the case of 14, the interaction is with the backbone amide.
[b] These distances are long for a hydrogen bond, but the direction is nearly ideal.
[c] The hydrogen bond has a rather poor geometry. The angle CA-N...OP1 is 88° in both cases.

Table 5. *Non-hydrogen bonding (hydrophobic) interactions between flavin ring and protein atoms less than 4.5 Å*[a]

Flavin Atom	Thr 56		Trp 57		Asn 58		Ile 59		Gly 60		Gly 89		Asp 90		Tyr 94		Asn 97		Phe 98		Gln 99	
	B	S	B	S	B	S	B	S	B	S	B	S	B	S	B	S	B	S	B	S	B	S
N1	0	1									2	0	2	1	0	3						
C2	1	3									2	0	2	0	0	3	2	0	2	0	1	0
O2	0	2									2	0	2	0	0	1	1	0	2	3	1	0
N3	1	2													0	2	1	1	1	0		
C4	2	2					2	0	1	0					0	4	2	1				
O4	0	2	1	0	1	0	2	0	1	0					0	3	1	2				
C4A	2	2	3	0			1	0							0	8						
N5	1	0	2	0	1	0									0	6						
C5A	1	0	2	1	1	0									0	7						
C6			2	2	2	1	1	0							0	5						
C7			0	2	0	3																
C7M			0	2	0	1									0	1						
C8			0	3											0	1						
C8M			0	2											0	1						
C9			0	4											0	3						
C9A	1	0													0	6						
N10	0	1													0	4						
C10A	2	0							1	0					0	4						

[a] For each residue, the numbers under B and S denote the number of interactions with backbone (B) and side chain (S) atoms, respectively.

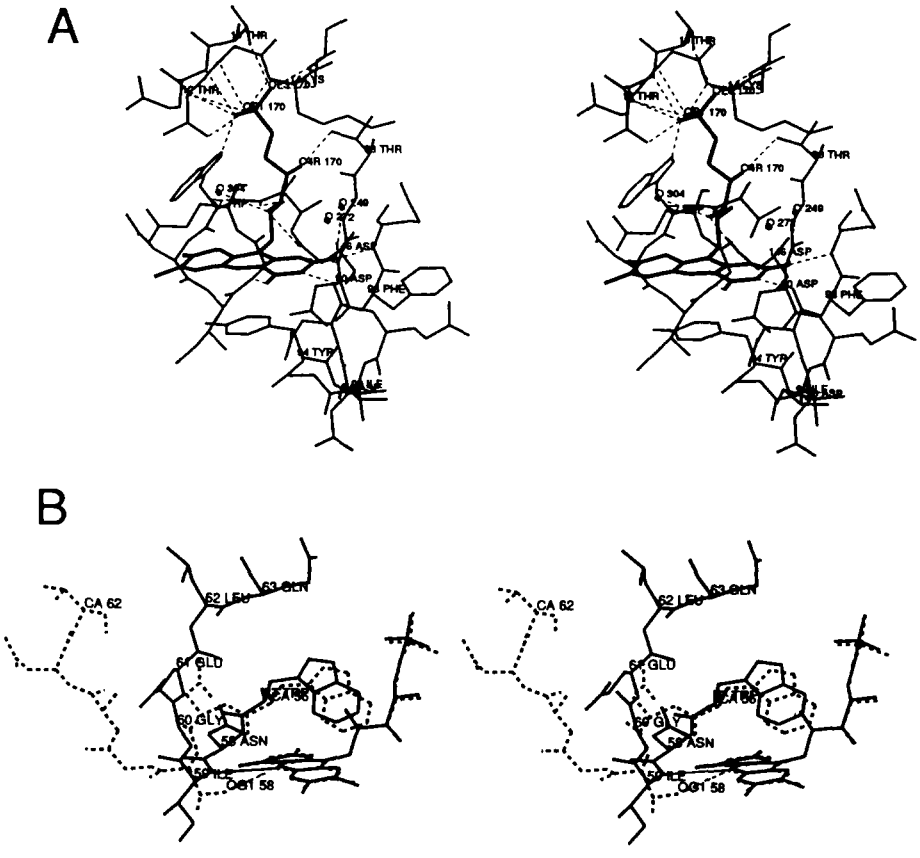

Fig. 7. Environment of FMN. **A:** All protein residues interacting with FMN in *Anabaena* 7120 are shown. The hydrogen bonds are shown as dashed lines. **B:** Comparison of the loop region interacting with N5 of the flavin ring. In *A.* 7120 (shown solid) the amide nitrogen of Ile 59 is at a distance of 3.6 Å but is in the plane of the flavin ring and pointing directly at N5 (connected as a thin line). In *Chondrus crispus* (shown dashed), the residue corresponding to 59 in *A.* 7120 is the nonhydrophobic Thr 58 and the side chain hydroxyl makes a hydrogen bond with N5 (thin dashed line) with a distance of 3.1 Å.

cated hydrogen bond with N1 and O2; the amide N of Gln 99 interacts with O2; the carbonyl O of Asn 97 hydrogen bonds to N3. Asp is an invariant residue at position 90 in all three long-chain flavodoxins and is involved in a hydrogen bond OD1 (Asp 90)... N (Gly 93) stabilizing this loop. The amide N of Gly 60 in the reverse loop makes a hydrogen bond with O4. No protein atoms or water molecules are within 3.2 Å of N5, the site of protonation upon reduction of flavin. The nearest protein atom is the amide N of Ile 59 at a distance of 3.6 Å. Even though this distance is long for a hydrogen bond, the geometry is good; it would normally be regarded as only a weak hydrogen bond. However, because this region is not solvent accessible, the interaction energy in vacuo, where the dielectric constant (ϵ) is closer to unity, can be higher (compared to aqueous environment where $\epsilon \approx 4$).

The flavin ring is bracketed by two aromatic side chains: Tyr 94 on one side, which is nearly parallel to the flavin ring with a dihedral angle of 8° and stacks on it, and Trp 57 on the other, which is tipped by 48°. In solution, this tyrosine was found to have a slower flip rate, presumably due to the additional hydrophobic interaction with the side chain of Ile 59 (Stockman et al., 1990).

It is seen (Tables 4, 5) that in the first loop consisting of residues 56–60, the interactions with the flavin ring are mostly to backbone atoms, whereas in the second loop consisting of residues 89–99, they are both to the backbone and side chain atoms. It is interesting that every atom of the flavin ring interacts with the side chain of Tyr 94, which is stacked on it (Kinemage 3). By contrast, Trp 57 brackets the flavin ring but is not stacked on it; its backbone interacts with the pyrimidine portion of the flavin ring, whereas its side chain interacts with the hydrophobic edge of the ring.

Comparison of FMN interactions in flavodoxins

Only minor differences are seen in hydrogen bonding interactions with FMN in the *A.* 7120 and *A. nidulans* flavodoxins. The ribityl hydroxyl O4′ interacts with the side chain hydroxyl of Thr 88 in *A.* 7120, whereas it interacts with a water molecule in *A. nidulans*. The water molecule W249 interacts with O2 of the flavin ring in *A.* 7120, whereas in *A. nidulans*, the equivalent water is slightly displaced and interacts with O4′ instead. In all three long-chain flavodoxins, the flavin ring is bracketed by the same residues and has similar interactions. The short-chain flavodoxin, *D. vulgaris*, also has the same aromatic residues bracketing the flavin ring. However, the short-chain flavodoxin from *C. beijerinckii* has only one aromatic side chain stacked on the flavin ring; Tyr 94 is replaced by Trp, whereas Trp 57 is substituted by Met, and the orientation of the flavin ring is different (see Fig. 6C).

The redox potential sq/rd is similar for all five flavo-

doxins, but the ox/sq value (≈ −200 mV) is lower for the long-chain flavodoxins than for short chains (≈ −100 mV) and is comparable to the value for free FMN (−238 mV). This may be rationalized by the presence of a hydrogen bond, in the oxidized state, to the N5 atom of the flavin from the amide NH of Ile 59 in *A.* 7120, from the amide NH of Val 59 in *A. nidulans*, or from the hydroxyl group of the side chain Thr 58 in *C. crispus*. This hydrogen bond is absent in the short-chain flavodoxins. The influence of the hydrogen bonding to N5 on the ox/sq value has also been independently noted (Fukuyama et al., 1992). In the short-chain flavodoxins, the transition from the ox to the sq state is accompanied by a conformational change in the loop residue, which is a Gly. In *C. beijerinckii* flavodoxin, for the mutants G57A, G57D, and G57N, the ox/sq values were lower (Ludwig et al., 1991), indicating that non-glycyl residues lower the value, but not all the way to the value found in the long-chain flavodoxins. In the long-chain flavodoxins, where an Asn replaces the Gly, the ox/sq value is further lowered probably because it is also coupled to the hydrogen bond to N5 present in the ox state. The hydrogen bond is with the peptide backbone NH in both *A.* 7120 and *A. nidulans*. The *C. crispus* flavodoxin, which has a similar ox/sq value, also has Asn 57, but the hydrogen bond is with the side chain of the nonhydrophobic residue Thr 58. The insertions in this loop in the *C. crispus* probably assist in positioning the side chain Thr 58 to form the hydrogen bond.

Solvent molecules

An α-carbon plot of the structure with the water molecules is shown in Figure 8A and B. A total of 104 water molecules were identified. Of these, 99 are in the first hydration shell, since they make at least one direct interaction with a protein atom, and 5 are in the second shell.

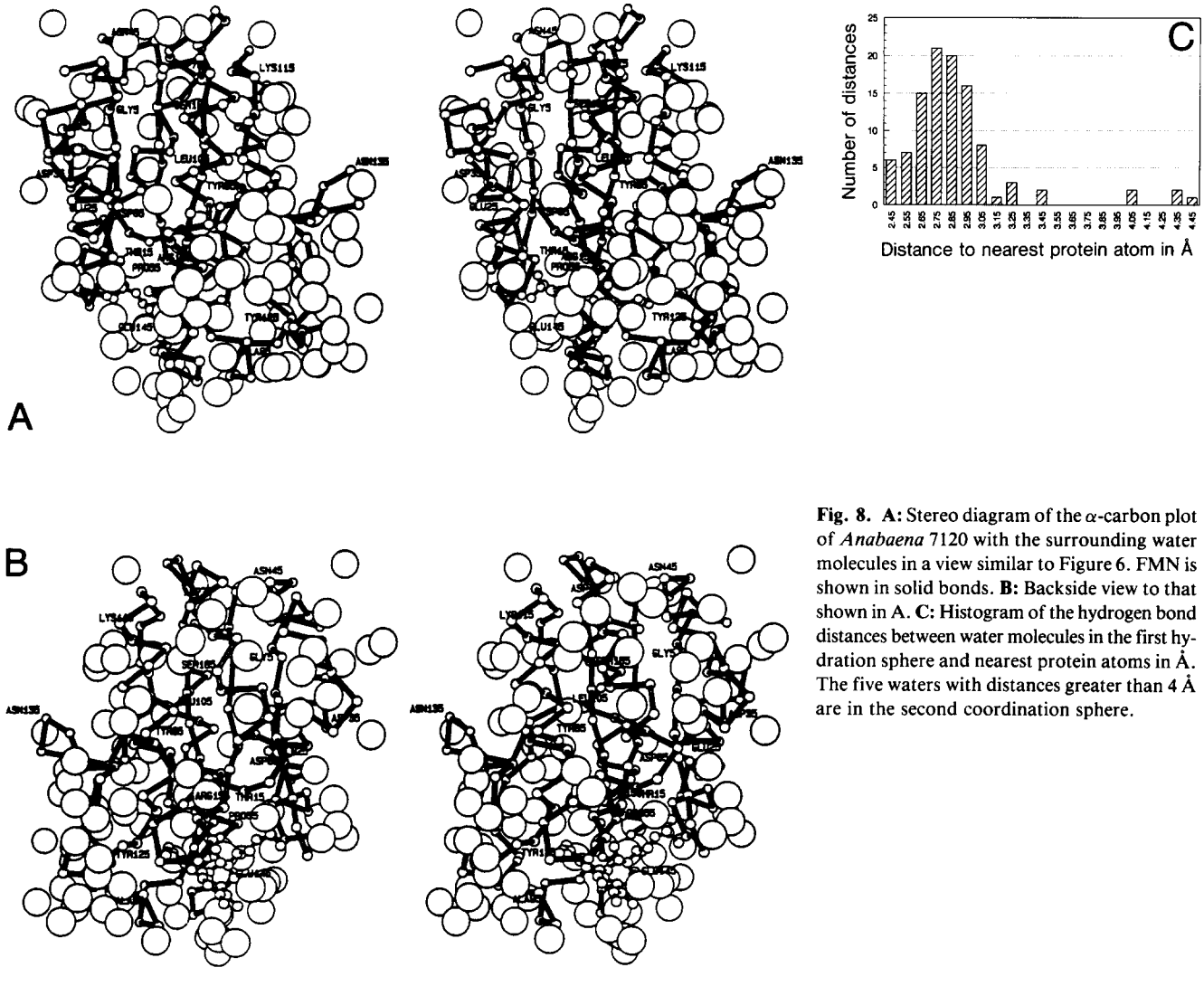

Fig. 8. A: Stereo diagram of the α-carbon plot of *Anabaena* 7120 with the surrounding water molecules in a view similar to Figure 6. FMN is shown in solid bonds. **B:** Backside view to that shown in A. **C:** Histogram of the hydrogen bond distances between water molecules in the first hydration sphere and nearest protein atoms in Å. The five waters with distances greater than 4 Å are in the second coordination sphere.

A histogram of the distances between water molecules in the first hydration shell, and the nearest protein atom with which they hydrogen bond is shown in Figure 8C. As expected, the distribution is clustered around 2.9 Å. Of the backbone atoms, 74 carbonyl oxygen atoms and 39 amide nitrogen atoms interact with water. Among the side chains, the largest number of interactions are found with Asp (47/20, i.e., 47 interactions to 20 Asp residues), Glu (19/11), Gln (13/10), and Ser (10/10). Asn, Arg, His, Lys, Thr, Tyr, and Trp have less than 10 interactions each. The trends observed here are similar to those seen in other proteins (Thanki et al., 1988). There are seven bidentate interactions with Asp (46, 75, 96, 100, 144, 153, and 154) and two with Glu (67 and 166). A water molecule (W236) bridges carbonyl O(3) and amide N(48) at the beginning of β-strands 1 and 3. Two water molecules hydrogen bond to atoms on FMN: O2...W249 and O3'...W304.

Water molecules contribute to a variety of intra- and intermolecular hydrogen bonds. All intramolecular water bridges are listed in Table 6. W236 forms a bridge between O(3) and N(48) at the beginning of the first and third β-strands. The interactions of residues in the α_2-helix region with W245, W275, W289, and the side chain of Arg 112 and its symmetry-related mate are shown in Figure 9A. W275 is inserted between O(71) and OD1 of Asp 74, which in turn, is bridged to O(70) via the water W245. These two waters are, in turn, bridged by a third water, W289. O(74) is engaged in an intramolecular hydrogen bond with NH2 of Arg 112. NH1 from a symmetry-related Arg 112, interacts with O(68) and OG of Ser 71. These water-mediated interactions result in this region being a loose 3_{10}-helix with only three hydrogen bonds: 70...73, 72...75, and 73...76. O(71) and N(74) are more than 3.5 Å apart. The region around residues 148–154, in the type I β-bend, are shown in Figure 9B and Kinemage 4. Here there is a network of waters, with W215 inserting between O(149) and OD1 of Asp 153 and W284 inserting between O(150) and N(154). The region of the

Table 6. *Intramolecular water bridges in Anabaena 7120*

W201	OH	(85 Tyr)	3.0 Å	OG1	(116 Thr)	2.8 Å				
W203	N	(96 Asp)	3.0	OD1	(97 Asn)	2.9				
W205	N	(149 Ser)	2.9	OG	(149 Ser)	2.5				
W206	OE2	(25 Glu)	2.6	O	(157 Lys)	2.9				
W207	OD1	(96 Asp)	2.9	N	(136 Gly)	2.7				
W209	O	(54 Cys)	2.8	OG1	(56 Thr)	2.8				
W210	N	(85 Tyr)	2.8	O	(117 Val)	2.6	O	(139 Val)	2.8 Å	
W212	N	(10 Thr)	3.0	OD2	(35 Asp)	2.8	OD2	(65 Asp)	2.7	
W215	O	(149 Ser)	2.7	N	(153 Asp)	3.0	OD1	(153 Asp)	2.8	
W216	O	(96 Asp)	2.9	OD1	(129 Asp)	2.9				
W217	O	(91 Gln)	2.8	OD2	(126 Asp)	2.8	O	(126 Asp)	2.8	
W220	OG1	(152 Thr)	3.0	NH1	(155 Arg)	2.7				
W222	OH	(70 Tyr)	2.5	O	(104 Leu)	2.8				
W224	N	(119 Tyr)	2.9	OE1	(166 Glu)	2.9				
W226	O	(93 Gly)	2.9	N	(95 Ala)	2.9				
W227	OD1	(96 Asp)	3.0	N	(135 Asn)	2.7				
W232	OG	(149 Ser)	2.6	O	(154 Asp)	2.8				
W236	O	(3 Lys)	2.9	N	(48 Glu)	2.8				
W237	N	(62 Leu)	2.9	OE2	(67 Glu)	2.7				
W240	O	(122 Thr)	2.6	O	(125 Tyr)	2.8				
W244	OD1	(100 Asp)	2.9	OD2	(100 Asp)	2.9				
W245	O	(70 Tyr)	2.8	OD1	(74 Asp)	2.9				
W248	O	(131 Lys)	2.7	O	(133 Leu)	2.7				
W249	OG1	(56 Thr)	2.7	O	(88 Thr)	2.7				
W252	O	(107 Glu)	2.8	OG	(110 Ser)	2.7				
W253	N	(122 Thr)	2.8	OG1	(122 Thr)	3.0	O	(136 Gly)	3.0	
W256	OG	(37 Ser)	2.7	NE2	(38 Gln)	2.9				
W257	O	(37 Ser)	3.0	O	(37 Ala)	3.0				
W260	O	(89 Gly)	2.3	OD2	(144 Asp)	2.7				
W268	OE1	(11 Gln)	2.5	NE2	(11 Gln)	3.0				
W269	ND1	(34 His)	2.8	OD2	(43 Asp)	3.0				
W270	OD1	(100 Asp)	2.7	NZ	(131 Lys)	2.5				
W271	OE2	(145 Glu)	3.0	OD1	(154 Asp)	2.4				
W272	O	(89 Gly)	2.6	OD1	(146 Asp)	2.4				
W273	NE2	(91 Gln)	2.8	OD2	(144 Asp)	2.5				
W275	O	(71 Ser)	2.6	OD1	(74 Asp)	2.9				
W280	OD1	(154 Asp)	2.9	OD2	(154 Asp)	2.6				
W284	O	(150 Asp)	2.8	N	(154 Asp)	3.0				
W287	O	(67 Glu)	2.9	O	(68 Gly)	3.0	OG	(71 Ser)	2.7	
W289	O	(71 Ser)	2.9	OD2	(75 Asp)	3.0				
W297	O	(19 Ala)	2.9	N	(23 Gln)	3.0				
W303	OE1	(72 Glu)	2.8	OD1	(75 Asp)	2.7				

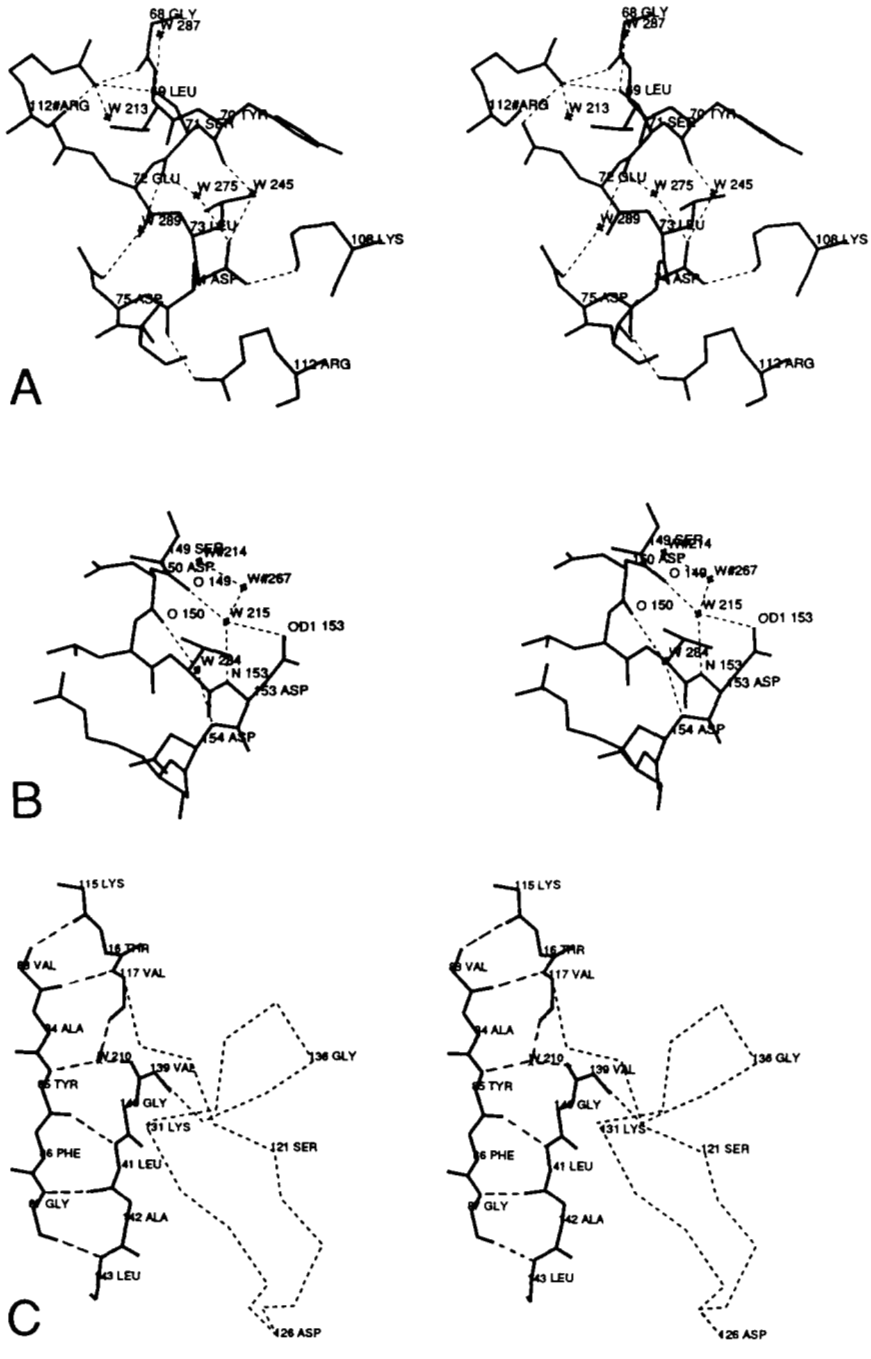

Fig. 9. Illustrations of water interactions: **A:** Region of the α_2-helix. Arg 112 of the reference molecule is at the bottom right and its NH2 forms a hydrogen bond with the carbonyl O of Asp 74. Arg 112 of a screw-related molecule is at top left and its NH1 participates in hydrogen bonding with carbonyl O of Gly 68, side chain hydroxyls of Ser 71 and Glu 72, and also W 213. **B:** Region 149–154. W 284 inserts between the carbonyl O(150) and amide N(154) and W215 between O(149) and N(153) and also forms a hydrogen bond with OD1 (Asp 153). The distance between W 215 and W 284 is 3.3 Å. **C:** Region of β_4–β_5 and the inserted water. The long loop in the middle of β_5 is on the right (dashed lines).

β_4 and β_5 sheets is shown in Figure 9C and Kinemage 2. The β_5-sheet is interrupted by the insertion of the long loop, residues 119–138. After the N(117)...O(83) sheet hydrogen bond, O(117) is linked to N(85) via water molecule W210. A similar water bridge is found in the other two long-chain flavodoxin structures. After the chain makes the excursion through the loop, O(139) latches onto the same water, W210. This neck region of the long loop is further stabilized by a short one-residue antiparallel β-strand between residues 120 and 138. The regular hydrogen bonding between β_4 and β_5 resumes with the N(141)... O(85) hydrogen bond after the turn. Thus, the hydrogen bonding pattern from the atoms on the β_4 strand is not interrupted.

Crystal packing

Each molecule of *A.* 7120 flavodoxin is surrounded by four screw axes that create large solvent channels of about 20 Å diameter running through the crystal, as viewed down the *b*-axis (Fig. 10). The direct intermolecular hydrogen bonds between protein atoms are listed in Table 7. There is a hydrogen bond between OE1 (Gln 10) and ND2 (Asn 135) of the molecule translated along the *b*-axis.

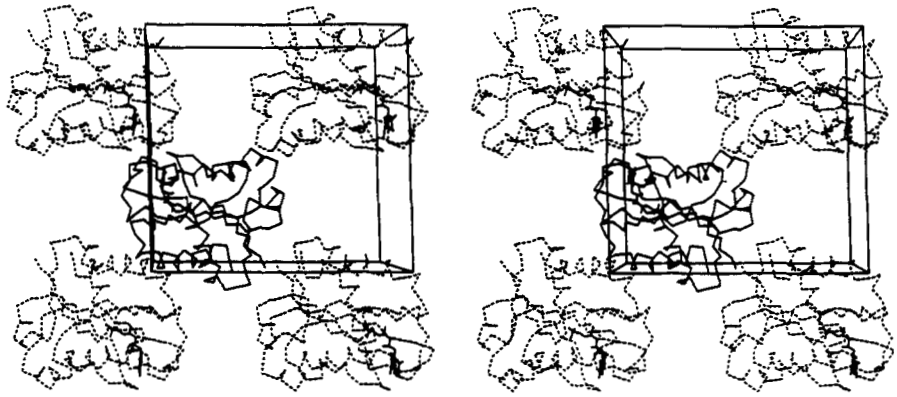

Fig. 10. Packing diagram of *Anabaena* 7120 flavodoxin as viewed down the *b*-axis. The *c*-axis is horizontal and the *a*-axis is vertical with the origin at left hand bottom corner. Notice the solvent channels that run along the *b*-axis between the molecules.

This region of the long loop is displaced in *A.* 7120, with reference to *A. nidulans* flavodoxin where there is no similar interaction. The closest packing of adjacent molecules is in three of the four corners in the *ac*-plane. Around the screw axis at (0,0), the α_4 helices of neighboring molecules come close; around the screw at $(\frac{1}{2},0)$ there is a hydrogen bond (2.7 Å) between OH (Tyr 94) of one molecule and OD1 (Asp 129) in the long loop of its neighbor. The residues 57–60 of the flavin binding region also butt against the residues 127–130 of the long loop of the neighbor. The interaction between the α_2-helix residues and the side chain of Arg 112 related by the screw at $(\frac{1}{2},\frac{1}{2})$ has already been described (Fig. 9A).

Comparison with NMR studies

Multinuclear NMR studies of *A.* 7120 flavodoxin (Stockman et al., 1990) provided partial identification of the secondary structure and a model for the FMN binding site. The NMR results are in substantial agreement with the present X-ray structure. Resonances were identified from all β-sheet residues except 3–4, 30–32, and 48. Because the first two of these regions did not provide well-defined electron density, this may indicate that they are mobile in solution and in the crystal. The position of the Trp 57 and Tyr 94 rings that bracket the flavin ring, as well as the groups that interact with the ribityl chain, are in good agreement. Although the flavin ring appears planar in the X-ray work, NMR data suggest that the xylene component is nonplanar. NMR data indicate that the carbonyl edge of the flavin is polarized by hydrogen bonding; the X-ray results indicate the H-bonds O2 . . . N (Gln 99), O2 . . . N (Asp 90), O4 . . . N (Gly 60). The hydrogen bond between N3 and O (Asn 97) (Table 4) was anticipated by NMR results. However, the NMR results did not indicate hydrogen bonding to N1, whereas a 3.0-Å distance was found between N1 and N (Asp 90) in the X-ray structure. More extensive comparisons will be possible once the full NMR assignments are completed and analyzed (unpubl.). Earlier NMR studies had shown that the ^{15}N chemical shift of N5 in *A.* 7120 flavodoxin is similar to that of free FMN and different from that of other flavodoxins (Stockman et al., 1988), suggesting that N5 might be exposed to solvent. However, the partial NMR structure (Stockman et al., 1990) showed N5 to be solvent inaccessible as found in the X-ray structure. The unusual ^{15}N chemical shift of N5 may be related to the hydrogen bond with the amide of Ile 59, which, as mentioned above, could be stronger than is apparent from the longer than normal distance for a hydrogen bond.

Table 7. *Intermolecular hydrogen bonds between protein atoms*

Atom/residue 1		Atom/residue 2		Distance (Å)	Symmetry code[a]
OE1	11 Gln	ND2	135 Asn	2.9	1, 0 1 0
O	68 Gly	NH1	112 Arg	2.6	2, 1 0 1
OG	71 Ser	NH1	112 Arg	3.1	2, 1 0 1
OE2	72 Glu	NE2	111 Gln	2.9	2, 1 0 1
		NE	112 Arg	3.0	2, 1 0 1
		NH1	112 Arg	2.8	2, 1 0 1
OH	94 Tyr	OD1	129 Asp	2.6	2, 1 0 0

[a] Symmetry code is symmetry operation number and translations along a, b, c. Symmetry operation: 1 = x, y, z and 2 = $-x, \frac{1}{2}+y, -z$.

Materials and methods

Protein

Anabaena 7120 was grown in 70-L batches in an illuminated rocker box (Kojiro, 1985). The cells were isolated by centrifugation, and the flavodoxin was purified by the method of D.W. Krogmann and C. Harper (Harper, 1988) as described by Stockman et al. (1988).

Crystallization

For crystallization, a 0.5% flavodoxin solution was dialyzed in 0.15 M Tris-HCl (pH 7.2) with 1.75 M $(NH_4)_2SO_4$

and 1 mM NaN_3. Small crystals grew from the dialyzed protein solution in a hanging drop against a reservoir of 3 M $(NH_4)_2SO_4$ at room temperature. Upon seeding with these small crystals, large, dark orange, rod-shaped crystals could be grown in about 2 weeks, which diffracted to beyond 2 Å resolution. The cell constants and space group are given in Table 8.

Data collection

Intensity data to 2 Å resolution were collected at the CHESS synchrotron source with an oscillation camera on films from one large crystal measuring 0.2 × 0.2 × 1.0 mm. The crystal was mounted with the *b*-axis nearly along the capillary tube. A total of 43 three-film packs were exposed for 15 s each with oscillation ranges of 3.6 or 4.0°. The crystal was irradiated at three different regions by moving it in the beam along its length. The films were developed, digitized with an Optronics scanner in Dr. Paul Sigler's laboratory at the University of Chicago, and processed by using the program DENZO (Otwinowski, pers. comm.). The data set was 91% complete; it contained 9,795 independent reflections with an R_{merg} of 0.07 on intensities. Of these, 8,493 reflections with $I > 2\sigma$ were used in the analysis. The details are given in Table 8.

Table 8. *Crystal, data collection, and data reduction parameters for Anabaena 7120 flavodoxin*

Crystal data	
Crystal size	0.2 × 0.2 × 1.0 mm
Space group	$P2_1$, monoclinic
Cell constants	48.0 (1) Å rms deviations in cell
	32.0 (1) Å constants determined
	51.6 (1) Å from processing the oscillation films
	β = 92.0 (1)°
Asymmetric unit contains one protein molecule and FMN	
Matthew's coefficient	2.06 Å^3/D
Solvent content	39%
Data collection	
Oscillation camera and synchrotron source at CHESS	
Wavelength, λ = 1.56 Å	
Temperature, 4°	
Crystal-to-film distance, 60 mm	
43 photographs (three films/pack). For 1–21, oscillation range of 4° was used and for 22–43, 3.6°. An overlap of 0.4° between successive oscillation ranges was used.	
Crystal was irradiated at three different positions along its length by translating it along its length (film packs 1–17, 18–31, and 32–43)	
Data reduction	
Films digitized on Optronics scanner	
Processed with the program Denzo	
Partial reflections were rejected	
Total reflections recorded = 24,329	
Unique reflections = 9,795	
R_{merg} = 0.07 on intensities	
91% of all possible reflections at 2 Å recorded	
8,543 with $I > 2\sigma(I)$ used in the refinement	

Structure solution

The structure was solved by molecular replacement with the program MERLOT (Fitzgerald, 1988) by using the coordinates of the homologous *A. nidulans* flavodoxin, provided by Dr. Martha Ludwig. The radial distribution of α-carbon distances in the model suggested that a radius of integration of 23 Å would be appropriate. The rotation function, which used 605 reflections in the 6–4-Å resolution range and the protein atoms of the model without FMN, had its largest peak at 5.3σ and its next peak below 4σ (Fig. 11A). By using the orientation corresponding to the highest peak, a translation function was calculated to determine x and z. This map was very clean and unequivocal, with the highest peak at 6.7σ and the next peak below 3σ (Fig. 11B). Because the y-coordinate is arbitrary in this space group, the *A. nidulans* model was oriented and positioned in the *A.* 7120 crystal according to these parameters. There were no unusually short intermolecular contacts, and a difference electron-density map calculated at 3 Å resolution contained clear density for FMN, which had not been included in the molecular replacement calculations. This strongly indicated that the solution was correct. The 52 residues that were different in the *A. nidulans* model were changed to correspond to the *A.* 7120 sequence.

Structure refinement

The molecular replacement solution was improved by a rigid-body refinement with the XPLOR program (Brunger, 1988), which used 4,925 reflections in the 6–2.5-Å resolution range. This reduced the *R*-value from 0.44 to

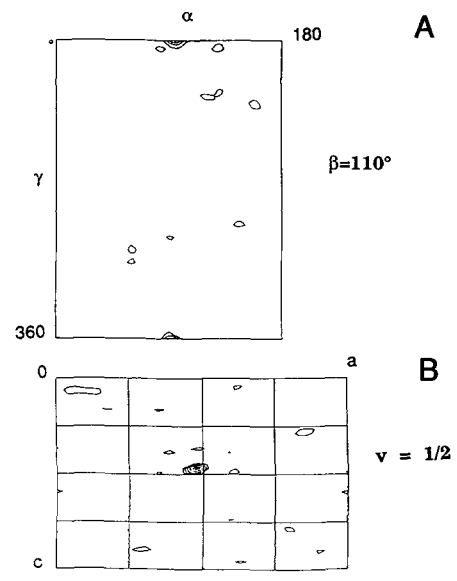

Fig. 11. Molecular replacement solution for *Anabaena* 7120 flavodoxin using *Anacystis nidulans* model. **A:** The section of the rotation function at $\beta = 110°$. **B:** Section $v = \frac{1}{2}$ of the translation function. In both maps, contours are at intervals of 1σ, starting at 2σ.

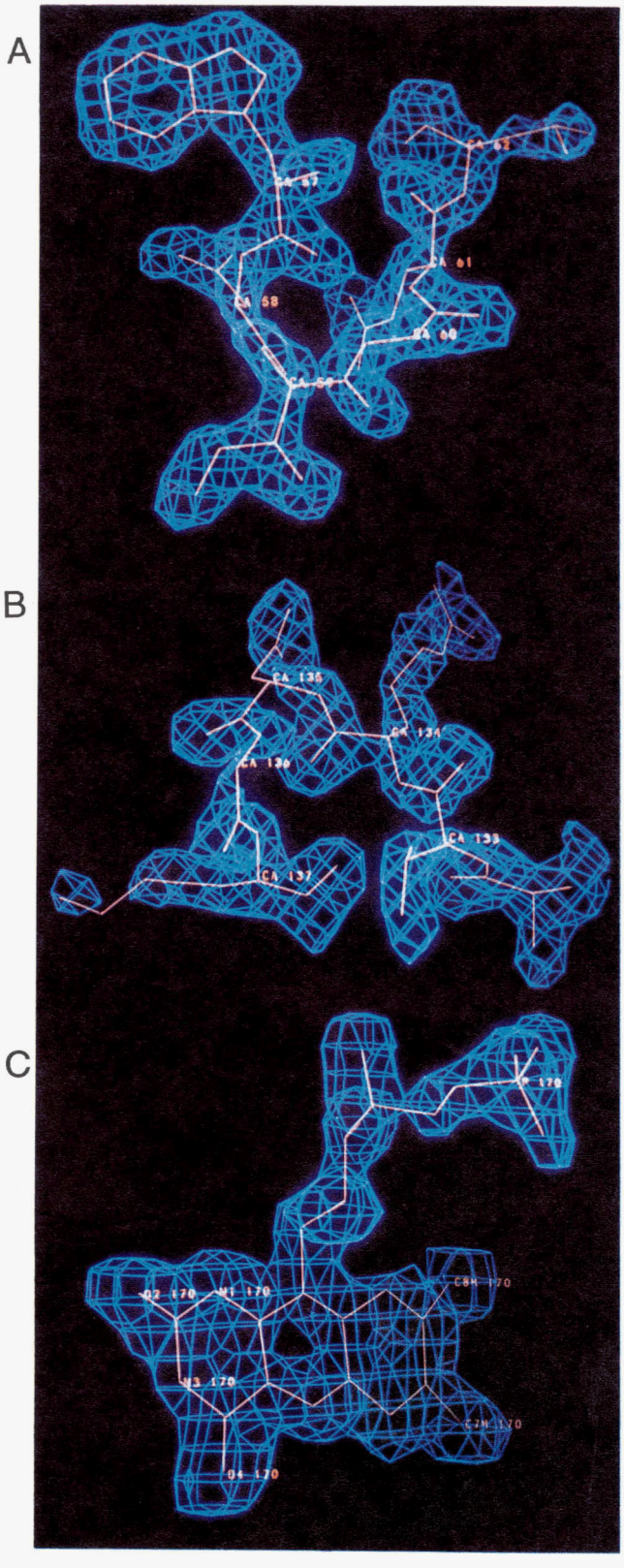

Fig. 12. Sim-weighted $2F_o - F_c$ omit electron density maps for *Anabaena* 7120 in color. **A:** Residues 57–62 of the FMN binding loop. **B:** Residues 132–137 of the long loop. **C:** FMN. The listed residues in A and B or FMN in C were omitted from phasing. Contours are drawn at 1.5σ.

0.37. Sim-weighted (Sim, 1960) $2F_o - F_c$ omit maps were calculated with phases from the protein atoms only, and FMN was fitted into the density by using the program FRODO (Jones, 1985) on the PS-300 graphics system. Residue 29 of the *A. nidulans* model, which is a deletion in *A.* 7120, was removed. The electron density in this region was very weak and disconnected, and it was not possible to rebuild across the gap. Therefore the loop was modeled to correspond to a type I turn (Richardson, 1981), as found in the short-chain flavodoxins. A round of simulated annealing refinement was performed by initially heating the system to 2,000°. This reduced the *R*-value to 0.23. The data resolution was increased to 2 Å to include all 8,493 reflections. The model was repeatedly refitted into omit maps followed by conjugate gradient refinement with XPLOR, which led to an *R*-value of 0.24. Solvent molecules were included with unit occupancy if their density in the difference electron-density map was at least at the 2.5σ level and made meaningful contacts with either the protein atoms or the already established solvents. After four rounds of solvent selection, model refitting, and refinement, the final *R*-value was 0.185 for the final model containing residues 2–169, FMN, and 104 solvent molecules. The *R*-value without the solvent molecules was 0.236. Inclusion of 365 reflections in the low resolution range up to 6 Å resolution resulted in *R*-values of 0.217 and 0.260, respectively. The average error in the coordinates, as estimated from Luzzati plots (Luzzati, 1952), was about 0.2 Å. The rms deviation from ideality was 0.02 Å for bond lengths and 3° for bond angles. The coordinates and structure factors have been deposited (1FLV) with the Protein Data Bank (Bernstein et al., 1977).

The electron density was generally clearly defined over most of the residues. The electron density for the N-terminal residue was not visible and for residues 2 and 3 was discontinuous. The loop residues 27–30 continued to be in weak and discontinuous density and could not be fitted. Three omit maps, covering residues 57–61 of the FMN binding loop, residues 132–137 of the long loop, and FMN, are shown in Figure 12.

Acknowledgments

C.Y. was supported by an NIH Molecular Biophysics Training Grant GM-08293 and B.J.S. by the Cell and Molecular Biology Training Grant GM-07215. We thank Dr. Martha Ludwig for providing the coordinates of *A. nidulans* flavodoxin, Dr. Straus for the gene sequence, and Dr. Fukuyama for sending us a preprint of their paper on *C. crispus*. M.S. gratefully acknowledges partial support of this work from the chair endowed by the Regents of The Ohio State University. Sample preparation was supported by USDA/SEA grant 88-37262-3406 to J.L.M.

References

Bernstein, F.C., Koetzle, T.F., Williams, G.J.B., Meyer, E.F., Brice, M.D., Rogers, J.B., Kennard, O., Shimanouchi, T., & Tasumi, M. (1977). The Protein Data Bank: A computer-based archival file for macromolecular structures. *J. Mol. Biol. 112*, 535–542.

Brunger, A.T. (1988). Crystallographic refinement by simulated annealing. In *Crystallographic Computing 4: Techniques and New Technologies* (Isaacs, N.W. & Taylor, M.R., Eds.), pp. 126–140. Clarendon Press, Oxford.

Burnett, R.M., Darling, G.D., Kendall, D.S., LeQuesne, M.E., Mayhew, S.G., Smith, W.W., & Ludwig, M.L. (1974). The structure of the oxidized form of clostridial flavodoxin at 1.9 Å resolution. Description of the flavin mononucleotide binding site. *J. Biol. Chem. 249*, 4383–4392.

Fitzgerald, P.M.D. (1988). MERLOT, an integrated package of computer programs for determination of crystal structures by molecular replacement. *J. Appl. Crystallogr. 21*, 273–278.

Fukuyama, K., Matsubara, H., & Rogers, L.J. (1992). Crystal structure of oxidized flavodoxin from red alga *Chondrus crispus* refined at 1.8 Å resolution. Description of the flavin mononucleotide binding site. *J. Mol. Biol. 225*, 775–789.

Fukuyama, K., Wakabayashi, S., Matsubara, H., & Rogers, L.J. (1990). Tertiary structure of oxidized flavodoxin from an eukaryotic red alga *Chondrus crispus* at 2.35 Å resolution. *J. Biol. Chem. 265*, 15804–15812.

Harper, C. (1988). A comparative study of proteins isolated from *Microcystis aeruginosa*. M.S. Thesis, Purdue University, West Lafayette, Indiana.

Jones, T.A. (1985). Interactive computer graphics: FRODO. *Methods Enzymol. 115*, 157–171.

Kojiro, C.L. (1985). Nuclear magnetic resonance studies of the "Blue Copper" protein plastocyanin. Ph.D. Thesis, Purdue University, West Lafayette, Indiana.

Laudenbach, D.E., Reith, M.E., & Straus, N.A. (1988). Isolation, sequence analysis and transcriptional studies of the flavodoxin gene from *Anabaena nidulans* R2. *J. Bacteriol. 170*, 258–265.

Laudenbach, D.E., Straus, N.A., Pattridge, K.A., & Ludwig, M.L. (1987). Sequence and structure of *Anacystis nidulans* flavodoxin: Comparisons with flavodoxins from other species. In *Flavins and Flavoproteins* (Edmondson, D.E. & McCormick D.B., Eds.), pp. 249–260. Walter de Gruyter, New York.

Leonhardt, K.G. & Straus, N.A. (1989). Sequence of the flavodoxin gene from *Anabaena variabilis* 7120. *Nucleic Acids Res. 17*, 4384.

Ludwig, M.L. & Luschinsky, C.L. (1992). Structure and redox properties of clostridial flavodoxin. In *Chemistry and Biochemistry of Flavoenzymes* (Muller, F., Ed.), Vol. III, pp. 427–466. CRC Press, Ann Arbor, Michigan.

Ludwig, M.L., Pattridge, K.A., Eren, M., & Swenson, R.P. (1991). Structural characterization of site mutants of clostridial flavodoxin. In *Flavins and Flavoproteins* (Curti, B., Zanetti, G., & Ronchi, S., Eds.), pp. 423–428. Walter de Gruyter, Berlin.

Luzzati, V. (1952). Traitement statistique des erreurs dans la determination des structures cristallines. *Acta Crystallogr. 5*, 802–810.

Mayhew, S.G. & Ludwig, M.L. (1975). Flavodoxins and electron-transferring flavoproteins. *Enzymes 12*, 57–118.

Paulsen, K.E., Stankovich, M.T., Stockman, B.J., & Markley, J.L. (1990). Redox and spectral properties of flavodoxins from *Anabaena* 7120. *Arch. Biochem. Biophys. 280*, 68–73.

Priestle, J.P. (1988). RIBBON: A stereo cartoon drawing program for proteins. *J. Appl. Crystallogr. 21*, 572–576.

Richardson, J.S. (1981). The anatomy and taxonomy of protein structure. *Adv. Protein Chem. 34*, 167–339.

Rossmann, M.G., Liljas, A., Branden, C.I., & Banaszak, L.J. (1975). Evolutionary and structural relationships among dehydrogenases. In *The Enzymes* (Boyer, P.D., Ed.), Vol. II, pp. 61–102. Academic Press, New York.

Sim, G.A. (1960). A note on the heavy-atom method. *Acta Crystallogr. 13*, 511–512.

Simondson, B.J. & Tollin, G. (1980). Structure-function relations in flavodoxins. *Mol. Cell. Biochem. 33*, 13–24

Smith, W.W., Burnett, R.M., Darling, G.D., & Ludwig, M.L. (1977). Structure of the semiquinone form of flavodoxin from *Clostridium MP*: Extension of 1.8 Å resolution and some comparisons with the oxidized state. *J. Mol. Biol. 117*, 195–225.

Smith, W.W., Pattridge, K.A., Ludwig, M.L., Petsko, G.A., Tsernoglou, D., Tanaka, M., & Yasunobu, K.T. (1983). Structure of the oxidized flavodoxin from *Anacystis nidulans*. *J. Mol. Biol. 165*, 737–755.

Stockman, B.J., Krezel, A.M., Markley, J.L., Leonhardt, K.G., & Straus, N.A. (1990). Hydrogen-1, carbon-13 and nitrogen-15 NMR spectroscopy of *Anabaena* 7120 flavodoxin: Assignment of β-sheet and flavin binding site resonances and analysis of protein–flavin interactions. *Biochemistry 29*, 9600–9609.

Stockman, B.J., Westler, W.M., Mooberry, E.S., & Markley, J.L. (1988). Flavodoxin from *Anabaena* 7120: Uniform N-15 enrichment and hydrogen-1, nitrogen-15 and phosphorus-31 NMR investigations of the FMN binding site in the reduced and oxidized states. *Biochemistry 27*, 136–142.

Sykes, G.A. & Rogers, L.J. (1984). Redox potentials of algal and cyanobacterial flavodoxins. *Biochem. J. 217*, 845–850.

Thanki, N., Thornton, J.M., & Goodfellow, J.M. (1988). Distributions of water around amino acid residues in proteins. *J. Mol. Biol. 202*, 637–657.

Tollin, G. & Edmondson, D.E. (1980). Purification and properties of flavodoxins. *Methods Enzymol. 69*, 392–406.

Wakabayashi, S., Kimura, T., Fukuyama, K., Matsubara, H., & Rogers, L.J. (1989). The amino acid sequence of a flavodoxin from the eukaryotic red alga *Chondrus crispus*. *Biochem. J. 263*, 981–984.

Watt, W., Tulinsky, A., Swenson, R.P., & Watenpaugh, K.D. (1991). Comparison of the crystal structures of a flavodoxin in its three oxidation states at cryogenic temperatures. *J. Mol. Biol. 218*, 195–208.